Journal of Analytical and Applied Pyrolysis 105 (2014) 49–54

Contents lists available at ScienceDirect

Journal of Analytical and Applied Pyrolysis

journal homepage: www.elsevier.com/locate/jaap

From new simple aliphatic to aromatic heterocycles built from 2-chloroethylisocyanate

Ana Julieta Pepino, Walter José Peláez, Gustavo Alejandro Argüello *

INFIQC, Departamento de Físico Química, Facultad de Ciencias Químicas, Universidad Nacional de órdoba, Argentina

ARTICLE INFO

Article history:
Received 14 August 2013
Accepted 10 October 2013
Available online 20 October 2013

Keywords:
Gas phase thermal reactions
2-Chloroethylisocyanate
DFT-calculation
Pyrazynes
Imidazolidine-2-ones

ABSTRACT

New routes for gas phase thermal reactions of 2-chloroethylisocyanate are presented. They can be tuned by simply changing the material of the reactor and the temperature. Many interesting products are formed, including pyrazines and novel imidazolidine-2-ones. A comprehensive analysis that included high level ab-initio calculations has been carried out. Beyond the general agreement found with experimental results, the most relevant information is that, irrespective of the material of the reactor, all the products can be explained through a common unique key intermediate.

1. Introduction

Alkyl isocyanates have been known since 150 years and are widely employed in preparative chemistry. The high reactivity of the isocyanates is related to the low electron density of the central carbon. They undergo many reactions [1–7], as addition, insertion, cycloaddition, carbodiimide formation, oligomerization and polymerization reactions [8–11]. Reportedly, alkyl and aryl isocyanates are found to trimerize upon heating to 1,3,5-trisubstituted hexahydro-s-triazinetriones. Only highly substituted isocyanates, fail to trimerize under these conditions [12]. Final products coming from isocyanates include both flexible and rigid polyurethane foams, coatings, adhesives, elastomers, and fibers for applications as diverse as furniture, bedding transportation, building, construction, automotive, footwear and the production of nitrosoureas which are used clinically as antineoplasic agents [13,14]. In a previous work [15], we presented the thermal behavior in gas phase of 2-chloroethylisocyanate **1**, showing the existence of two different mechanisms, depending upon temperature, which were interpreted in terms of simple second- and first-order reactions, respectively. The proposed pathways were based on the gaseous products identified by FTIR which was the experimental technique used.

Later studies, carried out to unravel the non-volatile products and to shed light about the mechanisms operating, led us to perform new pyrolysis reactions with GC–MS detection. Surprisingly, the results showed that novel aliphatic imidazolidines as well as aromatic pyrazines are obtained as main products (though through complex mechanisms) but their presence definitely depends on the material of the reactor where the reaction is performed. These new findings conform the content of the present contribution.

2. Materials and methods

2.1. General

$ClCH_2CH_2NCO$ **1** was obtained from commercial source (Aldrich, 97%) and was manipulated in a glass vacuum line equipped with a capacitance pressure gauge, three U-traps and valves with PTFE stems (Young, London, UK). The sample was purified by repeated trap-to-trap condensation and its purity was checked by IR and (^{1}H, ^{13}C) NMR spectroscopy.

All compounds were characterized by standard spectroscopic techniques (^{1}H, ^{13}C NMR, HMBC, HSQC, UV, IR) and mass spectrometry, and all data are in agreement with the proposed structures. NMRs were recorded in acetone-d_6 with a Bruker Avance II 400 MHz spectrometer (BBI probe, *z* gradient) (^{1}H at 400.16 MHz and ^{13}C at 100.56 MHz). Chemical shifts are reported in parts per million (ppm) downfield from TMS. The spectra were measured at 22 °C. Absorption spectra of the solutions were recorded with a UV-1601 Shimadzu spectrophotometer using a quartz cell with an optical path length of 1 cm and acetonitrile as solvent. Infrared solid spectra were recorded with an FTIR Bruker IFS 28 spectrometer, with a resolution of 2 cm^{-1} in the range from 4000 to 400 cm^{-1} by using KBr disks. Gas chromatography/mass spectrometry (GC/MS) analyses were performed with a Shimadzu GC–MS-QP 5050

* Corresponding author. Tel.: +54 351 433 4169.
E-mail address: gaac@fcq.unc.edu.ar (G.A. Argüello).

0165-2370/$ – see front matter © 2013 Elsevier B.V. All rights reserved.
http://dx.doi.org/10.1016/j.jaap.2013.10.003

spectrometer equipped with a VF column (30 m × 0.25 mm × 5 μm) by using helium as eluent at a flow rate of 1.1 mL min^{-1}. The injector and ion source temperature was 280 °C, the oven heating ramp was 15 °C min^{-1} from 150 up to 280 °C, and the interface temperature was 280 °C. The pressure in the MS instrument was 10^{-5} Torr, precluding ion-molecule reactions from taking place, and MS recordings were made in the electron impact mode (EI) at ionization energy of 70 eV.

2.2. Calculations

All calculations were performed with the Gaussian 09 program system [16] by using a DFT-B3LYP/6-311++G(3df,3pd) approach. Transition-state theory was used to evaluate the energy of the different channels. The transition states were characterized by the presence of one negative frequency and the internal reaction's coordinate (IRC) method was applied to verify that the correct states were connected.

2.3. Static pyrolysis

Static pyrolyses were performed in a Vycor glass reactor by using a tube furnace with a temperature-controller device. The substrate (100 mL, 122 mg, 0.947 mmol) was introduced into a reaction tube (1.5 cm × 12 cm Pyrex), cooled in liquid nitrogen, sealed under vacuum (0.06 mbar) and then placed in the Vycor glass reactor during 5–60 min at 250 °C. For the reactions in presence of iron, approximately 5.0 g of iron wires of 3.0 cm of length were introduced in each reactor at 120–375 °C during 30 min. The resulting pale yellow oil of the pyrolizates were then extracted with solvent (acetone-d6) and subjected to purification by column chromatography [hexane, hexane/chloroform (5:5), chloroform, chloroform/ethanol (8:2), then ethanol].

2.3.1. 1,3,5-Tris(2-chloroethyl)-1,3,5-triazinane-2,4,6-trione (**2**)

8% yield at 250 °C and 20 min of reaction. MS (EI): *m*/*z* (%) = 315(M$^+$, 2), 282(41), 280(62), 268(11), 266(16), 246(1), 244(6), 218(6), 204(6), 177(2), 175(6), 168(21), 163(10), 161(26), 150(1), 148(2), 147(2), 125(3), 107(4), 105(8), 99(18), 70(66), 63(11), 56(100), 42(15).

2.3.2. (Z)-2-(3-(2-Chloroethyl)-2-oxoimidazolidin-1-yl)-N-(2-chloroethylidene)-2-oxoacetamide (**3**) and 1-(2-chloroethyl)-3-(4,5-dihydrooxazole-2 carbonyl)imidazolidin-2-one (**4**)

Isolated as a 39:71 mixture (measured by GC–MS), 29% yield at 250 °C and 20 min of reaction.

*2.3.2.1. Compound (**3**).* MS (EI): *m*/*z* (%) = 282(2), 280(M$^+$, 3), 253(2), 220(5), 218(16), 206(31), 204(94), 177(18), 175(42), 150(4), 149(2), 148(14), 147(3), 113(4), 99(100), 78(2), 70(30), 65(10), 63(34), 56(34), 42(23).

*2.3.2.2. Compound (**4**).* MS (EI): *m*/*z* (%) = 246(M$^+$, 5), 236(7), 216(17), 215(49), 203(17), 201(16), 187(8), 184(9), 174(9), 160(8), 149(70), 139(72), 132(8), 105(55), 96(33),82(100), 77(26), 70(23), 63(8), 56(23), 55(8), 53(7), 51(7), 42(24), 41(23), 40(22).

2.3.3. 1-(Aziridine-1-carbonyl)-3-(2-chloroethyl)imidazolidin 2-one (**5**)

19% yield at 250 °C and 60 min of reaction. ^{1}H NMR (400 MHz, acetone-d$_6$) δ = 3.59 (m, 6H), 3.66 (t, 2H), 3.76 (m, 4H) ppm. ^{13}C NMR (100 MHz, acetone-d6) δ = 40.4(×2), 42.1, 42.2, 44.4, 153.9, 157.7 ppm. MS (EI): *m*/*z* (%) = 220(5), 218(M$^+$, 16), 206(30), 204(92), 177(14), 175(42), 168(30), 150(4), 148(14), 99(100), 70(14), 63(31), 42(24). Uv V(CH3CN): $\varepsilon_{211} = (9.045 \pm 0.006)104\ M^{-1}\ cm^{-1}$. IR (KBr) = 2917.8, 2850.3, 1711.5, 1675.8, 1541.8, 1485.9, 1440.6, 1361.5, 1263.2, 755.9 cm^{-1}.

2.3.4. 1-(2-Chloroethyl)imidazolidin-2-one (**6**) CAS #: 2387-20-4

15% yield at 250 °C and 60 min of reaction. MS (EI): *m*/*z* (%) = 150(5), 148(M$^+$, 22), 113(27), 99(22), 86(100), 70(7), 63(8), 56(60), 55(37), 44(25), 42(27), 41(8), 40(5).

2.3.5. N-(2-Chloroethyl)aziridine-1-carboxamide (**7**)

5% yield at 250 °C and 60 min of reaction. MS (EI): *m*/*z* (%) = 148(M$^+$, 7), 99(100), 85(3), 70(19), 56(34), 42(16).

2.3.6. Ethyl 2-chloroethylcarbamate (**9**)

7% yield at 250 °C and 60 min of reaction. MS (EI): *m*/*z* (%) = 151(M$^+$, 4), 108(4), 106(11), 103(4), 102(100), 74(2), 65(6), 63(18), 44(11).

2.3.7. 2-Methylpyrazine (**18**) CAS #: 109-08-0

37% yield at 250 °C and 30 min of reaction, and 8% yield at 375 °C and 30 min of reaction. MS (EI): *m*/*z* (%) = 95(5), 94(M$^+$, 100), 67(56), 53(14), 52(7), 44(8), 42(8), 40(16), 39(16), 38(10), 36(12).

2.3.8. 2,3-Dimethylpyrazine (**19**) CAS #: 5910-89-4

36% yield at 375 °C and 30 min of reaction. MS (EI): *m*/*z* (%) = 109(8), 108(M$^+$, 100), 107(36), 93(3), 80(9), 67(81), 53(8), 52(9), 51(6), 42(15), 41(11), 40(20), 39(14), 38(5).

2.3.9. 2-Ethyl-3-methylpyrazine (**20**) CAS #: 15707-23-0

22% yield at 375 °C and 30 min of reaction. MS (EI): *m*/*z* (%) = 122(86), 121(M$^+$, 100), 107(4), 94(15), 80(20), 67(25), 52(9), 42(21).

2.3.10. 2,3-Diethylpyrazine (**21**) CAS #: 15707-24-1

14% yield at 375 °C and 30 min of reaction. MS (EI): *m*/*z* (%) = 136(95), 135(M$^+$, 100), 121(57), 120(7), 108(5), 107(18), 94(4), 93(3), 81(9), 80(24), 66(5), 57(15), 54(8), 53(8), 52(10), 51(4), 39(17).

2.3.11. 5-ethyl-2,3-dimethylpyrazine (**22**) CAS #: 13925-07-0

2% yield at 375 °C and 30 min of reaction. MS (EI): *m*/*z* (%) = 136(63), 135(M$^+$, 100), 108(12), 107(3), 93(2), 80(6), 67(3), 53(13), 39(18).

3. Results and discussion

3.1. Decomposition of 2-chloroethylisocyanate **1** in a glass cell

The identification of all reaction products from pyrolysis of **1** was carried out at 250 °C in a glass cell for different periods of time (5–60 min).

At short times of reaction, five products were obtained and identified as 1,3,5-tris(2-chloroethyl)-1,3,5-triazinane-2,4,6-trione **2**, 2-(3-(2-chloroethyl)-2-oxoimidazolidin-1-yl)-N-(2-chloroethylid-ene)-2-oxoacetamide **3**, 1-(2-chloroethyl)-3-(4,5-dihydrooxazole-2-carbonyl)imidazolidin-2-one **4**, 1-(aziridine-1-carbonyl)-3-(2-chloroethyl)imidazolidin-2-one **5** and 1-(2-chloroethyl)imidazolidin-2-one **6** (Scheme 1); while, at longer times, new predominant products, identified as N-(2-chloroethyl)aziridine-1-carboxamide **7**, ethanol **8** and ethyl 2-chloroethyl carbamate **9**, were obtained at the expense of the decrease in concentration of compounds **2**, **3**, **4** and **6**.

Scheme 1 illustrates mechanistic routes to the formation of **2**–**9** in a glass reactor. The first step involves dimerization of the reactant to give the key intermediate **11a** from which we can rationalize the whole mechanism: path A shows the equilibrium leading to the formation of the dimer **10**, which was not experimentally detected

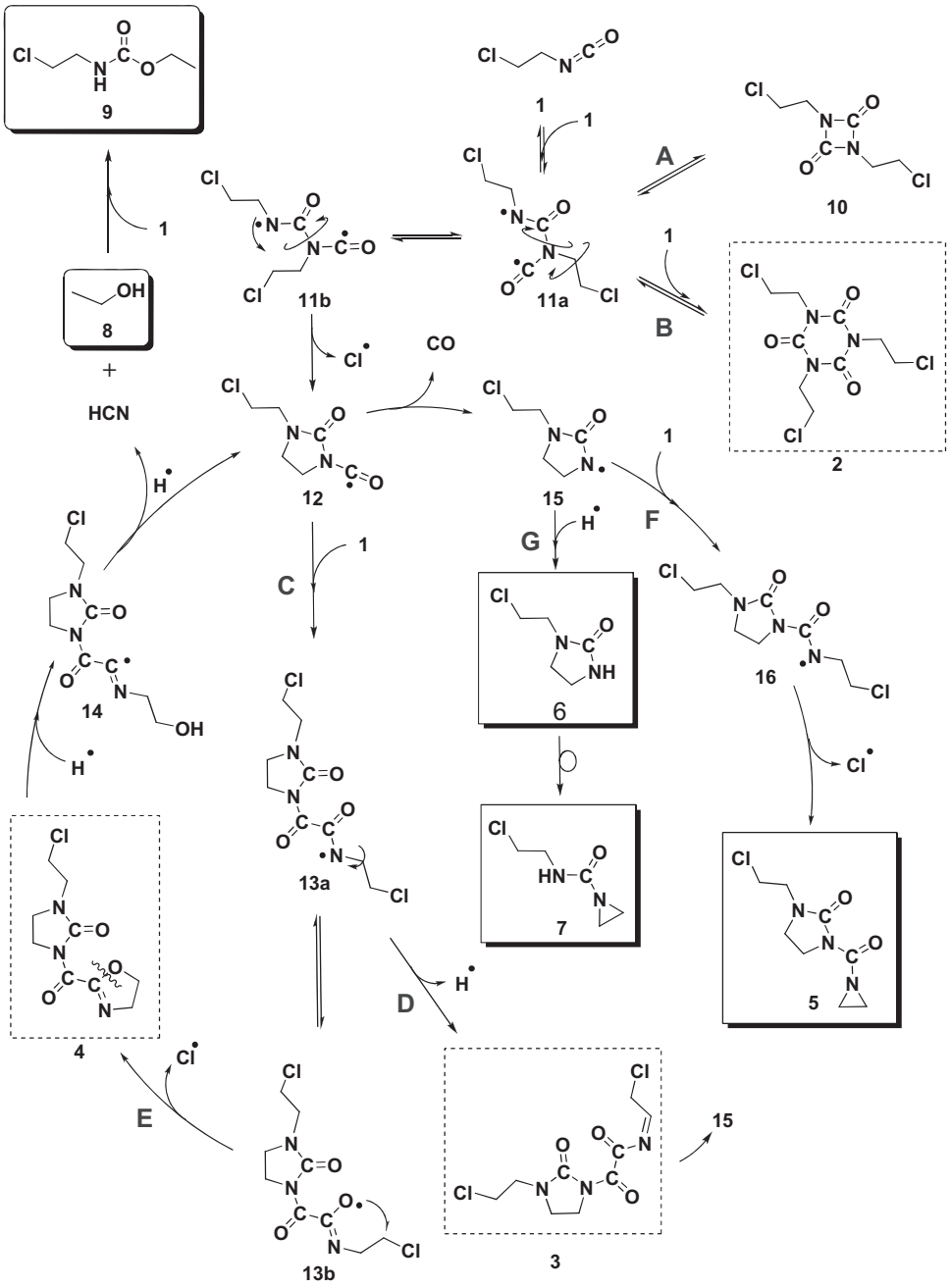

Scheme 1. Decomposition of 2-chloroethylisocyanate **1** in a glass cell. Dashed boxes: compounds obtained at intermediate times. Solid boxes: final products.

because it is consumed as the time elapses since, as will be shown later, the activation energy for the ring opening is small. Path B, leads to the formation of the trimer **2** through an equilibrium process that also explains why it decreases at longer times even though it is the most stable compound. Interestingly, **2** is the well-known end product of many previous studies on isocyanates [17,18].

Intramolecular cyclization of the rotamer **11b** allows the formation of all remaining products through the clue intermediate **12**. Though this intermediate seems to be unlikely, it is the responsible for the appearance of the detected species **3** and **4**, which have a carbonyl group that can only be explained by its existence. The coupling of **12** with a new molecule of reactant (path C) leads to **3** by hydrogen elimination (path D), or through a new intramolecular cyclization of **13** yields **4** (path E). On the other hand, **12** can lose CO to form **15** which, in turn, reacts with **1** yielding **5** through **16** (path F) or captures hydrogen to yield **6** (path G).

As time elapses, and the initial concentration of the reactant goes down, the channels needing more than one reagent molecule fade out surviving path G, from where **6** could rearrange to **7**. Thus, the final products remaining are **5**, **6**, **7**, **8** and **9**.

3.2. Calculation of the decomposition reaction of 2-chloroethylisocyanate *1* in gas phase

Calculations on the energetics of the whole mechanism, including moieties that were considered unstable for years, have been carried out for the first time. Different routes of reaction of the intermediate **11** were performed at DFT-B3LYP/6-311++G(3df,3pd) level. The formation of **10** and **2** demands less energy than the final product **5**. It is to note, that the formation of **2** (Fig. 1, blue line) releases a substantial amount of energy and therefore it

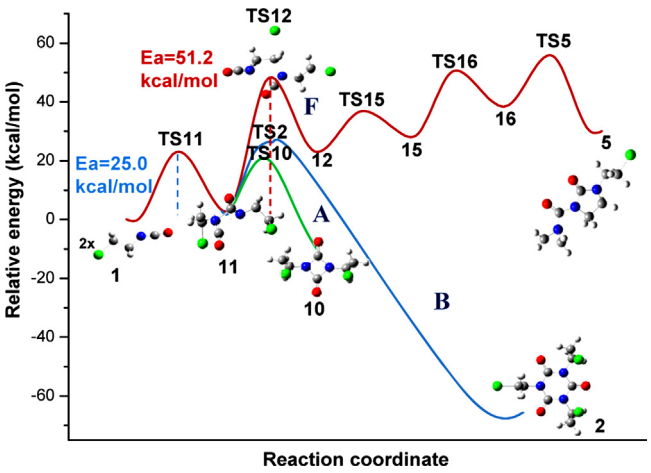

Fig. 1. Reaction coordinates for the formation of **2**, **5** and **10**. (For interpretation of the references to color in citations of this figure, the reader is referred to the web version of this article.)

accumulates supporting the old chemistry statements that alkyl isocyanates trimerize rather than dimerize [17,18].

Actually, the dimer **10** (Fig. 1, green line) should also be formed but the activation energy needed for the ring opening is only about 17 kcal mol^{-1}, and therefore it reacts further to give the other products. Real time experiments at short times should be carried out in order to prove the existence of the questioned dimer.

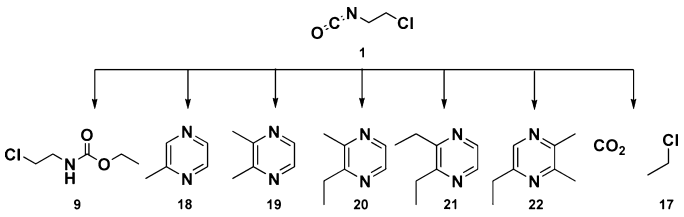

Scheme 2. Main products obtained in the thermolysis of **1** in presence of iron.

Compound **5** turned out to be a novel and stable heterocycle. It can be formed after the barrier of the **TS12** (51.2 kcal mol^{-1}) has been overcome (Fig. 1, red line). Loss of CO, coupling with a new molecule of reactant, loss of chlorine and cyclization to afford the final product **5** are less energy demanding paths (**TS15** = 12.7 kcal mol^{-1}, **TS16** = 21.4 kcal mol^{-1} and **TS5** = 16.0 kcal mol^{-1}, respectively).

For the processes that lead the products **3** and **4** (paths CD and CE, Scheme 1), the energy requirements are similar, being the rate determining step of the reaction the same as for **5** (Figure S1 in the supporting information).

3.3. Decomposition of 2-chloroethylisocyanate *1* in presence of iron

As stated before, the very nature of the products formed relies on the surface material of the reactor. While for the previous determinations of the FTIR in situ [15] we used steel, for static pyrolyses

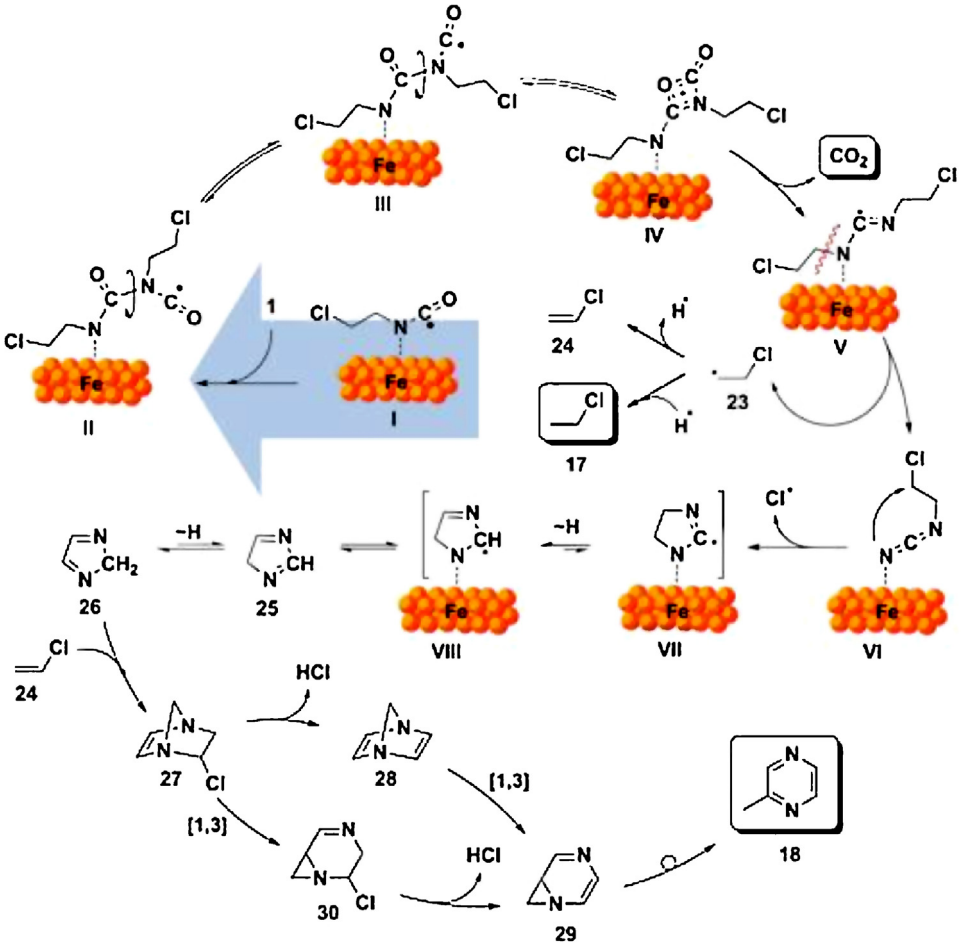

Scheme 3. Proposed mechanisms for the decomposition of **1** at low temperatures in presence of iron (120–260 °C).

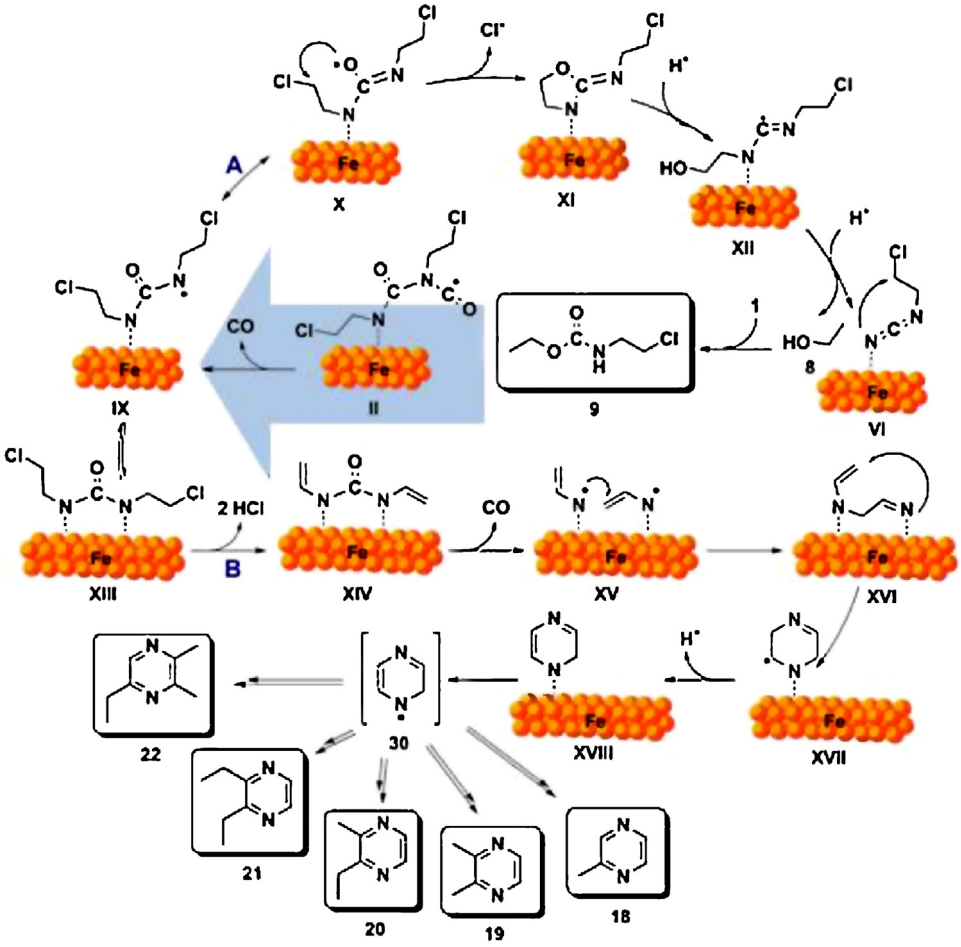

Scheme 4. Proposed mechanisms for the decomposition of **1** at high temperatures in presence of iron (260–375 °C).

were glass reactors. Thus, the results suggest that heterogeneous processes with the surface drive the reaction into other products.

The pyrolyses monitored by FTIR in situ [15] were performed in small scale steel reactors. Therefore, in order to isolate and purify bulk amount of products, we performed reactions in glass reactors filled with iron wool. These reactions were carried out using the same conditions of our previous work [15].

By analyzing the gaseous products we identified CO_2 and ethyl chloride **17** in the whole interval of temperatures, but at the higher temperatures HCl and CO were also detected. These results are in complete agreement with what we previously reported [15], though we did not observed **17** possibly due to its low concentration. Surprisingly, compounds **2**–**7** were not observed. Rather, substituted pyrazines **18**–**22** were identified as the main products of the reaction (Scheme 2).

The possible mechanism paths for the decomposition in the presence of iron at low (120–260 °C) and high (260–375 °C) temperatures are shown in Schemes 3 and 4, respectively. At any temperature, the first step consists in the adsorption of the reactant to the metal through the nitrogen atom (**I**). Later, a second molecule of **1** adds to **I** to form the dimer **II** which is still linked to the metal. Note that it is exactly the same as intermediate **11** but linked to the surface. At low temperature (Scheme 3), cyclization and losing of CO_2 gives the intermediate **V** from which radical **23** is obtained. This radical yields the identified product **17** and chloroethene **24** which reacts at a later stage providing the key step to the formation of pyrazines. The rest of the nitrogenated moiety still fixed to the metal **VI**, can rearrange and after desorption leads to the formation of **26**. At this stage reacts with **24** through the [4+2] cycloaddition to form the precursor of the pyrazine **18** by similar, simple and well-known rearrangements [19].

At higher temperatures (Scheme 4), intermediate **II** is more able to fragment (releasing CO) generating intermediate **IX** which can trigger the subsequent competitive routes, intramolecular cyclization–fragmentation (path A) and adsorption–dehydrochlorination (path B). The first ends up with the loss of an ethanol and intermediate **VI**. As mentioned before, ethanol adds to a reactant molecule giving **9**. The structure remaining linked to the metal (**VI**) gives product **18** as was explained in Scheme 3. Once intermediate **XIII** is formed (path B), it releases HCl to give **XIV** and CO leading to the very reactive intermediates **XV**, from where the pyrazine heterocycle can be formed through **XVI**–**XVIII**. Desorption of this structure explains the formation of the radical hydro-1,4-pyrazine (**30**) which, for instance, could recombine with radical **23** allowing the formation of the other pyrazines (**19**–**22**) after the loss of chlorine and hydrogen abstraction (Scheme 4).

This mechanism is in concordance with the observed by FTIR as CO_2 is the main gaseous product released at lower temperatures while HCl and CO form at higher ones [15].

4. Conclusions

The experiments described in the present paper account for a comprehensive knowledge of the reactions of 2-chloroethylisocyanate. Thus, both coarse and fine tuning of

the pyrolysis (surface reactor and temperature) conveys the reaction to very different products (aliphatic or aromatic heterocycles). Nevertheless all the mechanisms go through a fundamental species that would form irrespective of the reactor. That is the key intermediate 11 or II. Surface reactor drives the reaction to the obtainment of aliphatic imidazolidin-2-ones, present in many biologically active compounds [20–23] or pyrazines, part of many polycyclic compounds with biological or industrial significance [24]. Moreover, temperature tuning allows the modification of the selective yield of 2-methylpyrazine 18, which is the starting point to the formation of tubercular drugs [25], whose formation is maximized at low temperatures.

To the best of our knowledge, we have presented the first thorough calculation of the energetic of the reactions occurring in a glass surface where we proved the old statements about stability of dimer or trimer compounds. We have also shown that other structures should form, though their assessment must wait until proper experiments are performed.

Acknowledgements

Thanks are due for the financial support provided by CONICET, FONCyT and SECyT-UNC. A.J.P. thanks CONICET for a doctoral fellowship.

Appendix A. Supplementary data

Supplementary material related to this article can be found, in the online version, at http://dx.doi.org/10.1016/j.jaap.2013.10.003.

References

[1] R. Richter, H. Ulrich, in: S. Patai (Ed.), The Chemistry of Cyanates and their Thio Derivatives, John Wiley & Sons, Inc., New York, 1977, p. 619.
[2] J.K. Rasmussen, A. Hassner, Chem. Rev. 76 (1976), 389–389.
[3] H.J. Twitchett, Chem. Soc. Rev. 3 (1974) 209–230.
[4] A.J. Fornace, K.W. Kohn, H.E. Kann, Cancer Res. 38 (1978) 1064–1069.
[5] V.I. Gorbatenko, L.I. Samarai, Synthesis (1980) 85–110.
[6] H. Hagemann, Angew. Chem. 89 (1977) 789–796.
[7] H. Hagemann, Houben-Weyl-4th Edition: Kohlensaure-Derivate, G. Thieme, New York, 1983, pp. 182–183.
[8] L. Capuano, P. Boschat, H.W. Heyer, G. Wachter, Chem. Ber. 106 (1973) 312–316.
[9] H. Bredereck, G. Simchen, E. Goknel, Chem. Ber. 103 (1970) 236–244.
[10] A.E. Gurgiolo (to Dow Chemical), US Patent 4,268,683 (1981).
[11] J.L. Chitwood, P.G. Gott, J.C. Martin, J. Org. Chem. 36 (1971) 2228–2232.
[12] S.L. Trenbeath, A.M. Feldman, L.J. Nummy (to American Cyanamid), The Merck Index: An Encyclopedia of Chemicals, Drugs, and Biologicals, US Patent 4,377,530 (1983).
[13] S. Budavari, M.J. O'Neal, in: A. Smith, P.E. Heckelman (Eds.), Merck & Co, Whitehouse Station, NJ, 2001.
[14] T.P. Johnston, G.S. McCaleb, P.S. Opliger, J.A. Montgomery, J. Med. Chem. 9 (1966) 892–911.
[15] G.A. Martínez Córdoba, L.A. Ramos, S.E. Ulic, J.L. Jios, C.O. DellaVedova, J. Pepino, M.A. Burgos Paci, G.A. Arguello, M. Ge, H. Beckers, H. Willner, J. Phys. Chem. A 115 (2011) 8608–8615.
[16] M.J. Frisch, G.W. Trucks, H.B. Schlegel, G.E. Scuseria, M.A. Robb, J.R. Cheeseman, G. Scalmani, V. Barone, B. Mennucci, G.A. Petersson, H. Nakatsuji, M. Caricato, X. Li, H.P. Hratchian, A.F. Izmaylov, J. Bloino, G. Zheng, J.L. Sonnenberg, M. Hada, M. Ehara, K. Toyota, R. Fukuda, J. Hasegawa, M. Ishida, T. Nakajima, Y. Honda, O. Kitao, H. Nakai, T. Vreven Jr., J.A. Montgomery, J.E. Peralta, F. Ogliaro, M. Bearpark, J.J. Heyd, E. Brothers, K.N. Kudin, V.N. Staroverov, T. Keith, R. Kobayashi, J. Normand, K. Raghavachari, A. Rendell, J.C. Burant, S.S. Iyengar, J. Tomasi, M. Cossi, N. Rega, J.M. Millam, M. Klene, J.E. Knox, J.B. Cross, V. Bakken, C. Adamo, J. Jaramillo, R. Gomperts, R.E. Stratmann, O. Yazyev, A.J. Austin, R. Cammi, C. Pomelli, J.W. Ochterski, R.L. Martin, K. Morokuma, V.G. Zakrzewski, G.A. Voth, P. Salvador, J.J. Dannenberg, S. Dapprich, A.A. Daniels, O. Farkas, J.B. Foresman, J.V. Ortiz, J. Ioslowski, D.J. Fox, Gaussian 09 (Revision B.01), Gaussian, Inc., Wallingford, CT, 2010;
A.-R.B.A. El-Gazzar, H.N. Hafez, H.-A.S. Abbas, Eur. J. Med. Chem. 44 (2009) 4229–4258.
[17] A.A. Caraculacu, S. Coseri, Prog. Polym. Sci. 26 (2001) 799–851.
[18] S. Ozaki, Chem. Rev. 72 (1972) 457–496.
[19] R.F.C. Brown, in: H. Wasserman (Ed.), Pyrolytic Methods in Organic Chemistry: Application of Flow and Flash Vacuum Pyrolytic Techniques, Academic Press, New York, 1980, p. 148.
[20] G.V. De Lucca, P.Y.S. Lam, Drugs Future 23 (1998) 987–994.
[21] F. Heidempergher, A. Pillan, V. Pinciroli, F. Vaghi, C. Arrigoni, G. Bolis, C. Caccia, L. Dho, R. McArthur, M.J. Varasi, Med. Chem. 40 (1997) 3369–3380.
[22] G.A. Reichard, C. Stengone, S. Paliwal, I. Mergelsberg, S. Majmundar, C. Wang, R. Tiberi, A.T. McPhail, J.J. Piwinkski, N. Shih, Org. Lett. 5 (2003) 4249–4251.
[23] J.M. Kim, T.E. Wilson, T.C. Norman, P.G. Schultz, Tetrahedron Lett. 37 (1996) 5309–5312.
[24] M. Dolezal, K. Kralova, in: S. Soloneski, M.L. Larramendy (Eds.), Agricultural and Biological Sciences: Herbicides Theory and Applications, Wiley-VCH, Weinheim, 2011, pp. 10–20 (Chapter 27).
[25] J. Basak, N. Hardia, S. Saxena, R. Dixit, R. Dwivedi, S. Bhadauria, R. Prasad, Ind. Eng. Chem. Res. 46 (2007) 7039–7044.